THE ASTROPHYSICAL JOURNAL, 266:L5–L9, 1983 March 1

X-RAY OBSERVATIONS OF THE ANTENNAE (NGC 4038/39)

G. FABBIANO AND G. TRINCHIERI
Harvard-Smithsonian Center for Astrophysics
Received 1982 May 11; accepted 1982 October 28

ABSTRACT

The merging galaxies NGC 4038/39 were observed with the imaging proportional counter onboard the *Einstein Observatory* on two separate occasions, 12 months apart. The X-ray map seems to follow the optical contour of the two "heads," although a softer X-ray component with a different spatial distribution might be present. We interpret the harder component as being due to the integrated emission of single X-ray sources (like SNRs and X-ray binaries) in the two interacting galaxies. A harder point-like source might also be present in the contact region. The softer component could be thermal emission of gas heated by the interaction between NGC 4038 and NGC 4039. Moreover, a significant difference was observed between the two exposures. An additional X-ray source is present in the first image, but not in the second. If this source is associated with the Antennae, it could be either a very bright X-ray transient or a recent, optically undetected supernova.

Subject headings: galaxies: general — X-rays: sources

I. INTRODUCTION

The galaxies NGC 4038/39, nicknamed the Antennae because of their peculiar appearance, have attracted the attention of many astronomers. This system, one of the peculiar objects in Arp's (1966) catalog, was theoretically modeled by Toomre and Toomre (1972). They showed that the peculiar shape of the galaxy could be explained in terms of tidal interaction between two colliding spiral galaxies. The Antennae consists of two "heads," rich in bright knots and H II regions (Rubin, Ford, and D'Odorico 1970), and two long streamers. Radio emission was discovered associated with the central region of the system (Purton and Wright 1972). H I measurements (Huchtmeier and Bohnenstengel 1975) led to the confirmation that the two streamers are part of the system. A later H I interferometer map (van der Hulst 1979) shows that most of the H I is associated with the two heads and peaked between them. NGC 4038/39 were observed in X-rays for the first time with the *Einstein Observatory* IPC (imaging proportional counter, Giacconi *et al.* 1979) as part of a survey of peculiar galaxies (Fabbiano, Feigelson, and Zamorani 1982). That observation led to the detection of an X-ray source associated with the Antennae with L_x (0.5–3.0 keV) $\sim 1 \times 10^{41}$ ergs s^{-1} ($H_0 = 50$ km s^{-1} Mpc^{-1}). The data moreover suggested that this source was not compatible with a single point source.

Given the obvious astrophysical interest of the Antennae, a longer exposure was taken, again with the IPC, in order to map the X-ray emission with better statistics. The results of these two observations are the subject of this *Letter*.

II. OBSERVATIONS AND DATA ANALYSIS

a) *Integrated Quantities*

Table 1 summarizes the two observations of the Antennae. The *Einstein* sequence number is given, together with the dates of the observations; the effective exposure time on the source; the background-subtracted counts in the ($\sim$ 0.5–3.0) keV band attributable to the extended source associated with the Antennae and their statistical error; the (0.5–3.0) keV observed flux; the equivalent hydrogen-absorbing column due to our Galaxy (from Heiles 1975); and the (0.5–3.0 keV) emitted X-ray luminosity, calculated for a distance of 29 Mpc ($H_0 = 50$ km s^{-1} Mpc^{-1}). In all the fluxes quoted in this *Letter*, a 20% systematic error must be added to the statistical error because of the uncertainty on the spectral parameters. This includes the possibility that the equivalent hydrogen column is higher due to H I in the galaxies themselves (van der Hulst 1979).

Most quantities and their derivations are as discussed by Fabbiano, Feigelson, and Zamorani (1982). A reprocessing of I469 allowed us to recover $\sim$ 300 s of the observation that were originally missing due to lack of aspect solution. Moreover, both images were reprocessed with the latest instrument calibrations to have the most reliable spatial information. Extra care was also taken to choose the appropriate area of the image to include as many source photons as possible.

Although the uncertain calibration of the IPC does not allow yet a sufficiently precise determination of the spectral parameters, it appears that a soft component is

TABLE 1

X-RAY OBSERVATIONS OF NGC 4038/39

Sequence Number (1)	Observation (year, day) (2)	Effective Exposure Time (s) (3)	Source Counts (4)	f_x(0.5–3.0 keV) (ergs cm^{-2} s^{-1})[a] (5)	N_H (cm^{-2}) (6)	L_x(0.5–3 keV) ($H_0 = 50$) ergs s^{-2} (7)
I469.....	1979, 172	1652	48.8 ± 7.9[b]	$(7.8 \pm 2.01) \times 10^{-13}$	3×10^{20}	7.7×10^{40}
I7054.....	1980, 166	5534	171.7 ± 16.7[c]	$(7.8 \pm 1.7) \times 10^{-13}$	3×10^{20}	7.7×10^{40}

[a] The error on the fluxes includes the 20% error due to the uncertainty in the spectral parameters.
[b] These counts do not include the counts in the NE quadrant (see text) that can be attributable to a variable point source.
[c] The total number of counts including those in the soft component (energies < 0.5 keV) is 219.2 ± 19.2.

present in the X-ray spectrum of the Antennae. The hardness ratio for I7054, calculated as in Fabbiano, Feigelson, and Zamorani (1982), is $R = 0.57 \pm 0.11$, smaller than the average ($R = 1.0$) found for late-type peculiar galaxies, and excess counts over the background level are present starting from the second PHA (pulse height analyzer) channel ($E \gtrsim 0.2$ keV). We comment later on the spatial distribution of the "soft" and the "hard" photons.

By comparing the radial extent of the image of sequence I7054 with the radial extent of a strong point source (3C 273), we find that the X-ray source is not consistent with a point source (a χ^2 test gives a probability $P \leq 1 \times 10^{-5}$). Forcing a fit to a two-dimensional Gaussian with the method discussed by Henry *et al.* (1979), we obtain a $\sigma = 0.'8 \pm 0.'1$ in the ~ 0.5–3.5 keV range. However, this is only a rough approximation since the X-ray maps (see § I*b*) show significant X-ray emission from a much wider angular area. The Gaussian fit is obviously affected by the rather peaked, harder X-ray emission in the centroid region. We find that the X-ray centroid is at R.A. (1950) = $11^h59^m20^s$, decl. (1950) = $-18°36'00''$. The uncertainty on this position is ~ 30″.

b) *Spatial Distribution of the X-ray Emission in the Two Different Observations*

To study the spatial distribution of the X-ray emission in I469 and I7054, we produced contour maps by two different methods: (*a*) by smoothing the data with a Gaussian of $\sigma = 45''$ to reduce the noise due to statistical fluctuations; (*b*) by a maximum entropy deconvolution (Willingale 1981; Van Speybroeck 1981, private communication). This latter method attempts to give a representation of the real source as free as possible from both noise and instrumental effects. In both cases the background was calculated away from the the central part of the image and subtracted from the contours. In the smoothed maps, contours starting from the 3 σ level over the background are plotted. Since it is not possible to assign a meaningful statistical value to the contours in the case of the maximum entropy deconvolution, we chose the first contour to give approximately the same noise level as the 3 σ contour in the smoothed maps.

A comparison of the contour maps of the two observations (Fig. 1, Plate L1) shows that I469 presents a NE component (both in the PHA 5–10 map shown in Fig. 1 and in the PHA 2–10 map) that is absent from the contour maps of I7054. To investigate the significance of this difference, we performed a χ^2 test between the two images using the PHA 2–10 maps, which have a higher number of photons, so as to maximize the statistical significance of our results. We binned the data in 8 × 8 pixels bin (64″ × 64″) using the same centroid, in R.A. and decl., for the two images ($11^h59^m19^s.0$, $-18°35'5''$). All the counts from the X-ray source were then divided in four quadrants (NE, NW, SW, and SE). We used the longer exposure as a template, and we normalized the shorter exposure to it, by the ratio of the background counts. We obtain that the probability of the two images being statistically compatible is $P = 3.6 \times 10^{-3}$. All the difference arises from the NE quadrants, the other three quadrants giving a probability $P = 8\%$.

The counts above background (PHA 2–10) in the NE quadrants of I469 and I7054 are listed in Table 2, along with the corresponding X-ray fluxes calculated using the exposure times from Table 1. The ratio of the fluxes shows that the NE quadrant of I469 yields 3.5 ± 0.9 times more X-ray flux than the NE quadrant of I7054. This result is significant at the 3.9 σ level. By subtraction, we find that the excess flux in the NE quadrant of I469 is (0.5–3.0 keV) $f_x \sim 2.1 \pm 0.9 \times 10^{-13}$ ergs cm^{-2} s^{-1} (significant at the 2.6 σ level; the error in f_x quoted here includes also the 20% error due to the uncertainty in the spectrum and instrument calibration). Dividing the longer exposure (I7054) in two pieces of equal length and performing a χ^2 test, we obtained that the probability that the two observations are not different is $P \approx 20\%$, thus showing that no significant changes occurred during this second exposure.

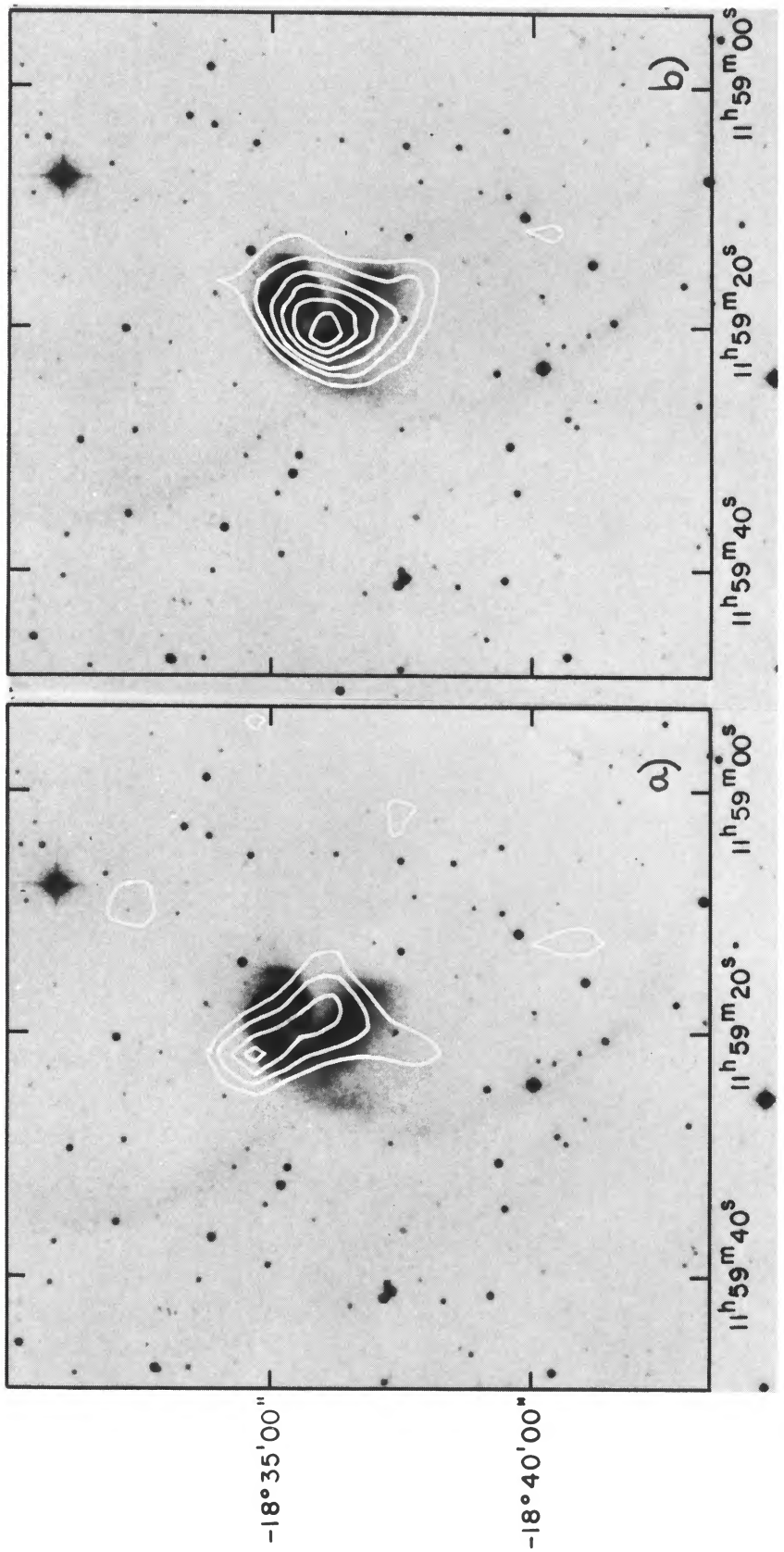

FIG 1.—Maximum entropy maps of PHA 5–10 (~ 0.7–2.8 keV) of (*a*) I469 and (*b*) I7054 superposed onto the optical image of NGC 4038/39 from the POSS plate

FABBIANO AND TRINCHIERI (*see* page L6)

TABLE 2

THE SOURCE IN THE NE QUADRANT

Sequence No.	Counts	(0.5–3.0 keV) f_x[a] (ergs cm^{-2} s^{-1})
I469	18.2 ± 4.7	(2.8 ± 0.9) × 10^{-13}
I7054	17.6 ± 5.7	(8.0 ± 3.0) × 10^{-14}

[a] The exposure times used to derive these fluxes are listed in Table 1. The errors in the fluxes include the 20% error due to the uncertainty in the spectral parameters.

c) *Spatial Distribution of the X-ray Emission of I7054 in Different Energy Ranges*

Since I469 and I7054 are statistically different, we did not add them together to derive a longer exposure map. Figures 2*a*–2*f* show the smoothed and maximum entropy maps for I7054 in three different energy ranges [PHA channels 2–4 (~ 0.2–0.7 keV), 5–10 (~ 0.7–2.8 keV), and 2–10 (~ 0.2–2.8 keV)]. The IPC beams shown in the figure were obtained using an IPC image of a strong point source (3C 273). The beams shown in the smoothed maps (Figs. 2*a*, 2*b*, and 2*c*) correspond to the first contours (3 σ) shown on the maps of the Antennae. To compare the maximum entropy maps to maps obtained from point sources yielding a similar number of counts, we divided the 3C 273 image into many such smaller pieces and ran the maximum entropy deconvolution on all of them. We found that, although the maps so obtained all had approximately the same diameter (which is the one we used for the beams in Figs. 2*d*, 2*e*, and 2*f*), small-scale structures within that diameter were present. We could not find any systematic effects in these features. We, therefore, conclude that small-scale structures in the maximum entropy maps (comparable with the maximum entropy beam size) are not to be trusted.

We notice that the contour maps from different PHA channels look different from each other. In particular, the soft map (PHA 2–4) does not seem to show a strong contribution from the region of the strong centroid of the PHA 5–10 map. Restricting ourselves only to the hardest photons (PHA 8–10), the image (not shown in the figure) is consistent with a point source at the position of the centroid. However, given the limited statistics and the different instrumental background and angular resolution at different energies, we find a probability $P = 4.3\%$ that the soft image and the PHA 8–10 hard image are consistent with each other when we try to quantify this difference with a χ^2 test similar to the one described above. Such a test will not take into account the full information in the detailed surface brightness distribution but only the difference in the count rates from the four quadrants into which we divide the image. Moreover, given the spectral spread function of the IPC, the different spectral channels are not truly independent.

We also looked in the IPC field for possible X-ray counterparts for the four radio continuum sources tabulated by van der Hulst (1979). None were found.

III. DISCUSSION

a) *Extended X-ray Emission of the Antennae*

As shown in the previous section, the overall X-ray emission associated with NGC 4038/39 is spatially extended, and it can be divided into at least two different components. The harder component ($E > 0.7$ keV) is responsible for the larger part of the total emission. As suggested by the PHA 5–7 (Fig. 2*f*) and PHA 5–10 (Fig. 1*b*) maximum entropy contour maps, this component seems to be associated with the two "heads." The centroid and the higher significance contours are associated with the impact region and a part of the southernmost head, both of which are particularly rich in H II regions (Boulesteix and Courtes 1978). This supports earlier findings that suggested an association between X-ray emission and the Population I galactic component (Fabbiano, Feigelson, and Zamorani 1982). Given the IPC spatial uncertainty (~ 30″), the centroid is also consistent with the region including knots C, D, and E of Rubin, Ford, and D'Odorico (1970). It might also be consistent with a point-like VLA source detected in this region (Ekers 1981, private communication). However, the general shape of the X-ray contours (see the maximum entropy map of Fig. 2*f*) seems to follow the shape of the optical emission, suggesting that a very significant fraction of the X-ray emission is probably due to the integrated contribution of unresolved galactic sources. The X-ray luminosity associated with the ~ 0.7–3.0 keV component is $L_x \sim 6 \times 10^{40}$ ergs s^{-1} for a distance $D = 29$ Mpc, about equally divided between the more extended component and the hard point-like source of PHA 8–10. The limited statistics of our data and the limited spatial and spectral resolution of the IPC do not allow us to explore in a more detailed and quantitative way the nature of the source at the X-ray centroid.

About 40% of the total source counts are in the PHA channels 2–4. This is not a common feature in peculiar late-type galaxies (Fabbiano, Feigelson, and Zamorani 1982). Although other possibilities are certainly open, one explanation for this emission is that of thermal emission from gas heated by shock fronts driven by the merging interaction. The total X-ray luminosity for the soft component is of the order of $L_{\rm gas} \sim 1 \times 10^{40}$ ergs s^{-1}. For a gas to irradiate in the 0.1–1.0 keV band, the temperature should be $T_{\rm gas} \sim 10^6$–10^7 K. This is also the temperature that can be derived by the velocity dispersion of the H I gas in the central position of the

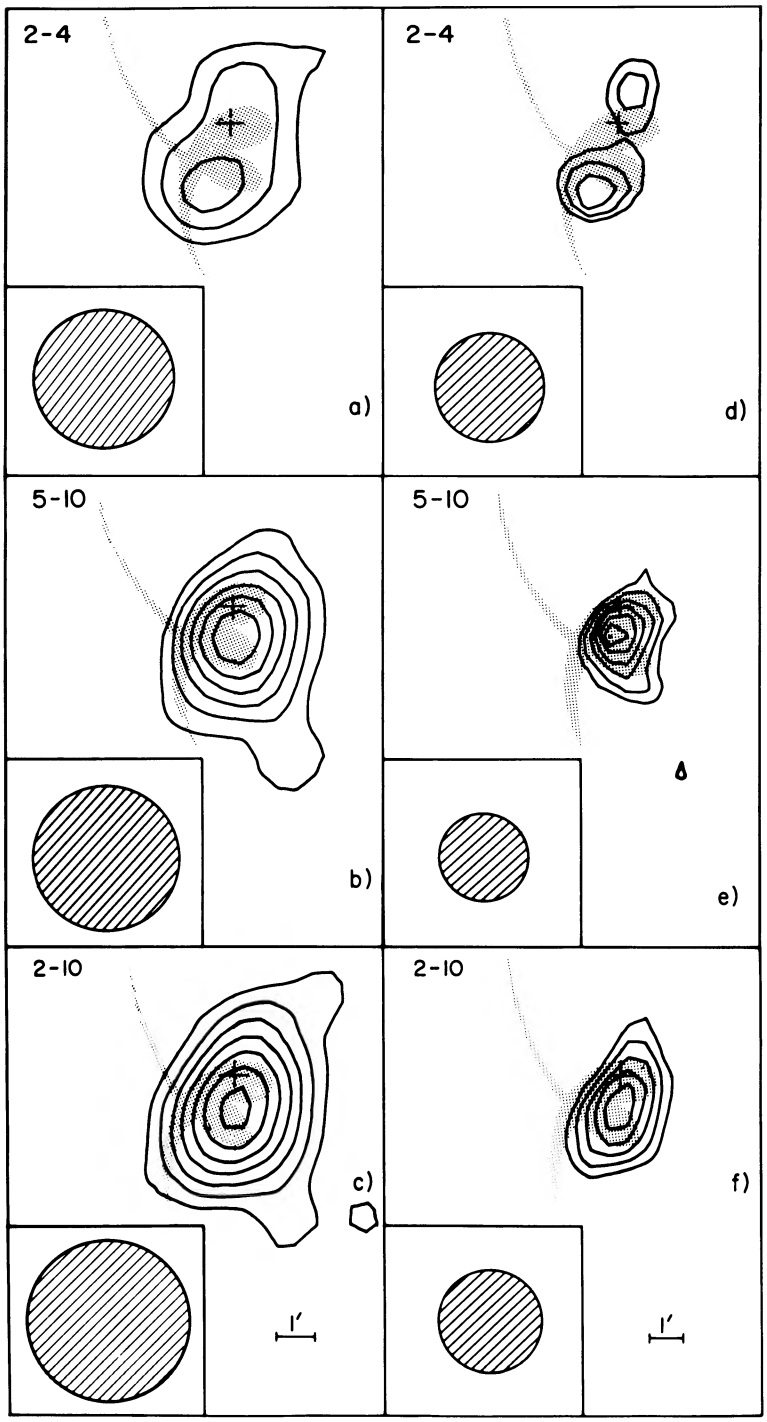

FIG. 2.—(*a*)–(*f*) The contour maps from PHA 2–4 (~ 0.2–0.7 keV), 5–10 (~ 0.7–2.8 keV), and 2–10 (~ 0.2–2.8) are shown for I7054. Maps (*a*), (*b*), and (*c*) were obtained by smoothing the data with a 45″ Gaussian. Maps (*d*), (*e*), and (*f*) are maximum entropy deconvolution maps. The first contour in the Gaussian smoothed maps is 3 σ over the background. The other contours follow in steps of 2 σ. The contours correspond to the following counts per square arc second: map (*a*) $(0.4, 0.8, 1.3) \times 10^{-3}$; map (*b*) $(0.4, 0.8, 1.2, 1.7, 2.3, 3.0) \times 10^{-3}$; map (*c*) $(0.6, 1.1, 1.6, 2.2, 2.9, 3.7, 4.5) \times 10^{-3}$. The first contours in the maximum entropy maps were chosen to minimize the noise level while still retaining enough information. North is at the top in all maps and east is on the left. The center of the cross superposed to the contour maps is at R.A. (1950) = $11^{h}59^{m}20^{s}$, decl. (1950) = $-18°35'5''$. The IPC beams (point response function) are shown in the insets. For a description of these beams, see text.

map of van der Hulst (1979). Given the limited statistics, it is impossible to give a firm estimate of the emitting volume. The maximum entropy map (Fig. 2*d*), however, shows X-ray emission extending as far as ~ 3′ from the impact region in the two (N and S) directions. Assuming a volume V_{gas} approximated by a sphere of 3′ radius, we can calculate the density of the gas from the equation $L_{gas} = 2 \times 10^{-27} N^2 V_{gas} T_{gas}^{1/2}$ (Tucker 1975), where N is the number of particles per unit volume. From here we obtain a mass of the X-ray emitting gas, $M_{gas} \sim 2 \times 10^9 M_\odot$, one order of magnitude more than the mass in the H I gas (van der Hulst 1979). The cooling time for this gas would be $\tau \sim 6 \times 10^9$ yr. If the emitting volume is as small as a sphere of 1′ radius, we obtain $M_{gas} \sim 4 \times 10^8$ and $\tau \sim 1 \times 10^9$ yr.

b) Transient Source in the NE Quadrant

As reported in the previous section, sequence I469 showed an excess count in the NE quadrant when compared with sequence I7054, suggesting a variable X-ray event in that part of the sky.

If this source were associated with the Antennae, its X-ray luminosity would be $L_x \sim 10^{40}$ ergs s^{-1}. It might be possible to explain such a high X-ray luminosity in terms of a transient binary X-ray source in the Antennae. An alternative possibility is a supernova event in the Antennae near in time to the first X-ray observation. By comparison with the X-ray flux detected by Canizares, Kriss, and Feigelson (1982) from SN 1980k in NGC 6946, we derive that the source in the Antennae, if a supernova, would be from ~ 16 to ~ 4 times (depending on the value of H_0, 50 or 100) brighter than SN 1980k.

However, it is most likely that the transient source in I469 is not associated with the Antennae. Based on the magnitude of the only object visible on the POSS plates in that area ($m \gtrsim 16$) and on considerations of X-ray to optical flux ratios, both a foreground star (see Vaiana *et al.* 1981) and a neutron star binary X-ray source can be excluded. A low-luminosity X-ray binary, like a cataclysmic variable, is a more likely candidate. The faintest such object detectable in ~ 5,000 s with *Einstein* would have $f_x \sim 3 \times 10^{-13}$ ergs cm^{-2} s^{-1} and $m \sim 16$ (Cordova and Mason 1982). Another possibility is a background variable QSO with $21 > m > 16$ (Zamorani *et al.* 1981). Optical work will be needed to check these two latter possibilities.

IV. CONCLUSION

The X-ray emission of the Antennae appears to have two components: a harder one, probably due to integrated emission from single X-ray sources in the two galaxies (like SNRs and binaries) and maybe also a strong hard point source in the impact region; and a softer one which could be indicative of hot gas in or near the impact region. If hot gas is present, the X-ray luminosity of the soft component suggests a mass of $M_{gas} \sim 10^8$–$10^9 M_\odot$, comparable to or higher than the mass present in H I.

We thank Alison Macdonald for assistance in the data reduction and Leon Van Speybroeck for a careful reading of the manuscript. We thank the CAL X-ray group for the use of their image of 3C 273 in our calibrations. G. T. acknowledges support from a C.N.R. fellowship. This work was supported under NASA contract NAS 8-30751.

REFERENCES

Arp, H. 1966, *Ap. J. Suppl.*, **14**, 1.
Boulesteix, J., and Courtes, G. 1978, *El Messagero, ESO Newsletter*, 1978 September.
Canizares, C., Kriss, G. A., and Feigelson, E. 1982, *Ap. J.* (*Letters*), **253**, L17 (Erratum 1982, *Ap. J.* [*Letters*], **258**, L83).
Cordova, F. A., and Mason, K. O. 1982, in *Accretion Driven Stellar X-ray Sources*, ed. W. H. G. Lewin and E. P. J. van Heuvel (Cambridge: Cambridge University Press), in press.
Fabbiano, G., Feigelson, E., and Zamorani, G. 1982, *Ap. J.*, **256**, 397.
Giacconi, R., *et al.* 1979, *Ap. J.*, **230**, 540.
Heiles, C. 1975, *Astr. Ap. Suppl.*, **20**, 37.
Henry, J. P., Branduardi, G., Briel, U., Fabricant, D., Feigelson, E., Murray, S., Soltan, A., and Tananbaum, T. 1979, *Ap. J.* (*Letters*), **234**, L15.
Huchtmeier, W. K., and Bohnenstengel, H.-D. 1975, *Astr. Ap.*, **41**, 477.
Purton, C. R., and Wright, A. E. 1972, *M.N.R.A.S.*, **159**, 15P.
Rubin, V. C., Ford, W. R., Jr., and D'Odorico, S. 1970, *Ap. J.*, **160**, 801.
Toomre, A., and Toomre, J. 1972, *Ap. J.*, **178**, 623.
Tucker, W. H. 1975, *Radiation Processes in Astrophysics* (Cambridge: MIT Press).
Vaiana, G. S., *et al.* 1981, *Ap. J.*, **245**, 163.
van der Hulst, J. M. 1979, *Astr. Ap.*, **71**, 131.
Willingale, R. 1981, *M.N.R.A.S.*, **194**, 359.
Zamorani, G., *et al.* 1981, *Ap. J.*, **243**, 357.

G. Fabbiano and G. Trinchieri: Harvard-Smithsonian Center for Astrophysics, 60 Garden Street, Cambridge, MA 02138